JMES The International Journal of
Mechanical Engineering and Sciences
https://iptek.its.ac.id/index.php/jmes
e-ISSN 2580-7471

KASITS: A Graphical User Interface for Kinematic Analysis and Synthesis of Five-Bar Linkage with Prismatic Joint

Taufik Ali Rahman[1], Achmad Saiful Hadi[1], Latifah Nurahmi[1], Ari K Saputra[1*], Bambang Pramujati[1], Unggul Wasiwitono[1], Arockia Selvakumar[2]

[1]Department of Mechanical Engineering, Institut Teknologi Sepuluh Nopember, Surabaya 60111, Indonesia
[2]School of Mechanical Engineering, Vellore Institute of Technology, Chennai, Tamil Nadu, India

Received: 16 September 2020, Revised: 2 January 2021, Accepted: 15 January 2021

Abstract

In this paper, a novel graphical user interface is developed for kinematic analysis and synthesis of five-bar linkage with prismatic joint, named KASITS. This interface has two menus that the users can freely select, namely for analysis and synthesis. In the analysis menu, the direct kinematics are derived to visually depict the overall workspace of the mechanism. Within this workspace, the singularity curves are plotted. In the synthesis menu, the value of design parameters is obtained for a given trajectory. An optimization is employed based on Pareto optimal solutions. The demonstration is provided to guide the users better.

Keywords: Graphical-user-interface, kinematics, analysis, synthesis, trajectories, singularities

1. Introduction

Five-bar linkage is a 2-Degree-Of-Freedom (DOF) mechanism that has simple structure. It makes five-bar linkage easier to be applied in industries, for example for pick-and-place operation. A new architecture of five-bar linkage was proposed in [1] by using non-circular gears therefore this mechanism is able to achieve a prescribed trajectory precisely. A planar five-bar linkage, dubbed DEXTAR (Dexterous Twin-Arm Robot), was developed in [2] to obtain a large workspace and to investigate the switching between working modes. The kinematic analysis that includes direct kinematics, inverse kinematics and singularities of five-bar linkage were discussed in [3]. A graphical user interface was proposed in [4] to carry out the structural synthesis of parallel manipulators with single platform. A new toolbox was developed in [5] based on MATLAB that has the capabilities like hand modelling, grasp definition, grasp modelling.

The solutions of direct kinematics will define the reachable point or workspace of mechanism. The workspace of 3-RPS cube mechanism is bounded by the Steiner surface [6] and if the axes of R-joints are rotated, the workspace changes into the Cross-cap surface [7]. The workspace size also changes depending on the value of design parameters [8]. The singularity analysis of a mechanism can be carried out by using Grassmann-Cayley algebra and the concept of wrench graph in [9] [10] [11] which become the main algorithm of a graphical user interface in [12]. The singularity of 3-DOF parallel mechanism has been computed and simulated in ADAMS in [13].

A novel graphical user interface was developed by [14] to guide the users for drawing several types of objects by using five-bar linkage, for example circle, line and square. The accuracy of the mechanism motion was validated through experimental tests. A methodology for type synthesis of 2-DOF mechanism with hybrid structure was proposed in [15] based on the Screw theory in [16]. By applying this procedure, several novel structures of 2-DOF hybrid mechanisms were developed, for example IRSBoT [17].

In this paper we have developed a graphical user interface for the kinematic analysis and synthesis of five-bar linkage with prismatic joint, named KASITS. This tool will provide two menus for the users to be selected, namely analysis and synthesis. In the analysis menu, the singularity curves are displayed within the mechanism workspace. The five-bar linkage studied in this paper comprises of four R-joints (R stands for Revolute) and one P-joint (P stands for Prismatic), and is used as an automatic catwalk in petroleum industry as shown in Figure 1. Automatic catwalk is used to transfer a tubular pipe from pipe rack onto rig floor.

2. Geometric Model of Five-Bar Linkage with P-Joint

The automatic catwalk depicted in Figure 1 is made up of five-bar linkage with prismatic joint. Its geometric model is shown in Figure 2. This mechanism is composed of two legs. The first leg of length l_2 is composed of RR joints which are denoted by points A and B.

*Corresponding author. Email: arikurniawans@me.its.ac.id

Figure 1. Five-bar linkage with P-joint for Automatic catwalk

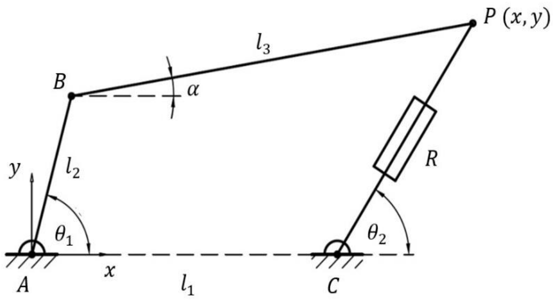

Figure 2. Geometric Model

The second leg is composed of RPR joints which are denoted by points C and P . The prismatic length is defined by R . The two legs are connected by the platform of length l_3 which becomes the bed of automatic catwalk. The angles of joints A , B and C are defined by θ_1 , α and θ_2 respectively. The output is measure from the coordinate of point P as (x, y).

3. Kinematic Analysis and Synthesis

Kinematic analysis of a mechanism is carried out in this paper to define the workspace, the solutions of direct kinematics and singularity curves for given values of design parameters. On the other hand, kinematic synthesis conducted in this paper aims to determine the value of design parameters for given trajectories by using the inverse kinematics. The initial step for the kinematic analysis and synthesis is to derive the position vector equations of mechanism based on Figure 2, as follows:

$$\overline{AP} = \overline{AB} + \overline{BP} \tag{1}$$

$$\begin{bmatrix} x \\ y \end{bmatrix} = \begin{bmatrix} l_2 \cos(\theta_1) \\ l_2 \sin(\theta_1) \end{bmatrix} + \begin{bmatrix} l_3 \cos(\alpha) \\ l_3 \sin(\alpha) \end{bmatrix} \tag{2}$$

$$\overline{AP} = \overline{AC} + \overline{CP} \tag{3}$$

$$\begin{bmatrix} x \\ y \end{bmatrix} = \begin{bmatrix} l_1 \\ 0 \end{bmatrix} + \begin{bmatrix} R \cos(\theta_2) \\ R \sin(\theta_2) \end{bmatrix} \tag{4}$$

In this paper, we provide two actuation schemes. The first actuation scheme is shown in Figure 3(a) where the actuators are mounted on R-joint and P-joint at points A and C, respectively. The variables of active joints are θ_1 and R. The second actuation scheme is depicted in Figure 3(b) where the actuators are attached on both R-joints at points A and R. The variables of active joint are thus θ_1 and θ_2. Each actuation scheme will produce different kinematic properties.

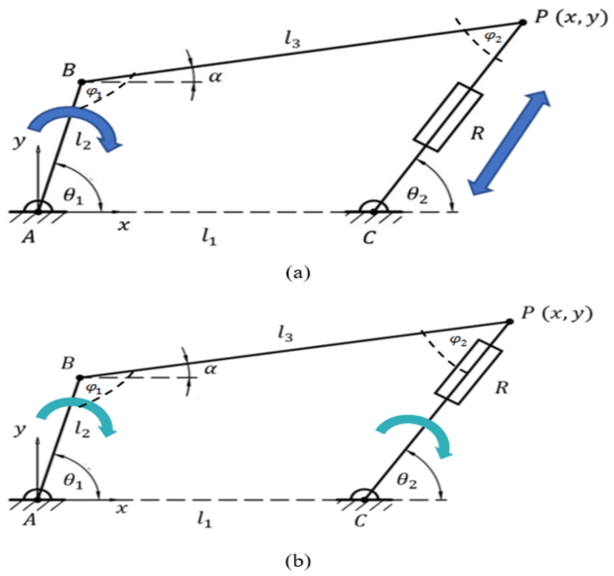

Figure 3. (a) Actuation scheme I, (b) Actuation scheme II

3.1. Direct Kinematics

By eliminating the variables of passive joints from Equation (2), the position of point $P\,(x,y)$ can be determined. For the first actuation scheme, the position of point $P\,(x,y)$ is a function of design parameters $l_1,\ l_2,\ l_3$ and joint variables θ_1, R as follows:

$$\begin{aligned} x = {} & ((2l_2^3l_1 - l_1^2l_2^2 - l_2^4 + l_2^2l_3^2 - l_2^2R^2)\cos^2(\theta_1) - (2l_1^3l_2 - 2l_1l_2l_3^2 + 2l_1l_2R^2)\cos(\theta_1) + l_1^4 + l_1^2l_2^2 + l_1^2l_3^2 - \\ & l_1^2R^2 \pm \sin(\theta_1)) - (-(4l_1^3l_2 - 4l_1l_2^3 + 4l_1l_2l_3^2 + 4l_1l_2R^2)\cos(\theta_1)4\cos^2(\theta_1)l_1^2l_2^2 + l_1^4 + 2l_1^2l_2^2 - 2l_1^2l_3^2 - \\ & 2l_1^2R^2 + l_2^4 - 2l_2^2l_3^2 - 2l_2^2R^2 + l_3^4 - 2l_3^2R^2 + R^4)(l_2\cos(\theta_1) - l_1)^2)^{\frac{1}{2}}l_2)/ \\ & 2(2l_2^2l_1\cos^2(\theta_1) - 3\cos(\theta_1)l_1^2l_2 - \cos(\theta_1)l_2^3 + l_1^3 + l_2^2l_1) \end{aligned} \tag{5}$$

$$\begin{aligned} y = {} & \frac{1}{2(2\cos(\theta_1)l_1l_2 - l_1^2 - l_2^2)}((2\cos(\theta_1)l_1l_2^2 - l_1^2l_2 - l_2^3 + l_2l_3^2 - l_2R^2)\sin(\theta_1) \mp (-(4\cos^2(\theta_1)l_1^2l_2^2 \\ & -(4l_1^3l_2 - 4l_1l_2^3 + 4l_1l_2l_3^2 + 4l_1l_2R^2)\cos(\theta_1) + l_1^4 + 2l_1^2l_2^2 - 2l_1^2l_3^2 - 2l_1^2R^2 + l_2^4 - 2l_2^2l_3^2 - \\ & 2l_2^2R^2 + l_3^4 - 2l_3^2R^2 + R^4)(l_2\cos(\theta_1) - l_1)^2)^{\frac{1}{2}}) \end{aligned} \tag{6}$$

The variables of passive joints from Equation (4) are eliminated hence the position of point $P\,(x,y)$ can be obtained. For the second actuation scheme, the position of point $P\,(x,y)$ is a function of design parameters $l_1,\ l_2,\ l_3$ and joint variables $\theta_1,\ \theta_2$ as follows:

$$\begin{aligned} x = {} & \cos(\theta_1)\cos^2(\theta_2)l_2 + \sin(\theta_1)\sin(\theta_2)\cos(\theta_2)l_2 - \cos^2(\theta_2)\ l_1 \pm (2\ \cos^2(\theta_1)\cos^2(\theta_2)\,l_2^2 + \\ & 2\cos(\theta_1)sin(\theta_1)\sin(\theta_2)\cos(\theta_2)l_2^2 - 2\ cos(\theta_1)\cos^2(\theta_2)\,l_1l_2 - 2\sin(\theta_1)\sin(\theta_2)\cos(\theta_2)l_1l_2 - \\ & \cos^2(\theta_1)\,l_2^2 + \cos^2(\theta_2)\left(l_1^2 - l_2^2\right) + 2\cos(\theta_1)l_1l_2 - l_1^2 + l_3^2)^{\frac{1}{2}}\cos(\theta_2)l_1 \end{aligned} \tag{7}$$

$$\begin{aligned} y = {} & (\cos(\theta_1)\cos(\theta_2)l_2 + l_2\sin(\theta_1)\sin(\theta_2) - \cos(\theta_2)l_1 \pm (\cos^2(\theta_1)\,l_2^2 + 2\cos^2(\theta_1)\cos^2(\theta_2)\,l_2^2\cos^2(\theta_2)\left(l_1^2 - l_2^2\right) \\ & -2\cos(\theta_1)\cos^2(\theta_2)\,l_1l_2 + 2\cos(\theta_1)\sin(\theta_1)\sin(\theta_2)\cos(\theta_2)l_2^2 - 2\sin(\theta_1)\sin(\theta_2)\cos(\theta_2)l_1l_2 + \\ & 2\cos(\theta_1)l_1l_2 - l_1^2 + l_3^2)^{\frac{1}{2}})\sin(\theta_2) \end{aligned} \tag{8}$$

3.2. Invers Kinematics

Inverse kinematics aims to find the solutions of the actuator displacements by eliminating the variables of passive joint. For the first actuation scheme, the aim is to find θ_1 and R, as follows:

$$\theta_1 = \tan^{-1}\left(\frac{A \mp B}{E}, \frac{C \pm D}{E}\right) \tag{9}$$

$$R = \sqrt{(l_1^2 - 2l_1x + x^2 + y^2)} \tag{10}$$

For the second actuation scheme, the purpose is to determine θ_1 and θ_2 , as:

$$\theta_1 = \tan^{-1}\left(\frac{A \mp B}{E}, \frac{C \pm D}{E}\right) \tag{11}$$

$$\theta_2 = -\tan^{-1}\left(y/\left(l_1 - x\right)\right) \tag{12}$$

Based on the value of joint angle θ_1 in Equations (9) and (11), there are two solutions of inverse kinematics. It means that link ABP has two configurations, namely solution 1 and solution 2 configurations.

where:

$$\begin{gathered}
A = {l_2}^2y - {l_3}^2y + x^2y + y^3 \\
B = x\sqrt{-{l_2}^4 + 2{l_2}^2{l_3}^2 + 2{l_2}^2x^2 + 2{l_2}^2y^2 - {l_3}^4 + 2{l_3}^2x^2 + 2{l_3}^2y^2 - x^4 - 2x^2y^2 - y^4} \\
C = {l_2}^2x - {l_3}^2x + x^3 + xy^2 \\
D = y\sqrt{-{l_2}^4 + 2{l_2}^2{l_3}^2 + 2{l_2}^2x^2 + 2{l_2}^2y^2 - {l_3}^4 + 2{l_3}^2x^2 + 2{l_3}^2y^2 - x^4 - 2x^2y^2 - y^4} \\
E = (x^2 + y^2)l_2
\end{gathered}$$

3.3. Singularities

A mechanism is said to be in singularities if the motions become suddenly uncontrollable and/or locked. Singularities may occur if the determinant of Jacobian matrix is null. There are two Jacobian matrices, namely inverse and forward Jacobian matrices which are called **A** and **B**, respectively. Jacobian matrices are formulated by deriving the position vector equations in Equations (2) and (4) with respect to time.

For the first actuation scheme (I), the Jacobian matrices $\mathbf{A_I}$ and $\mathbf{B_I}$ are determined as follows:

$$\mathbf{A_I}\begin{bmatrix}\dot{x}\\ \dot{y}\end{bmatrix} = \mathbf{B_I}\begin{bmatrix}\dot{\theta_1}\\ \dot{r}\end{bmatrix} \tag{13}$$

$$\mathbf{A_I} = \begin{bmatrix} x - \cos(\theta_1)l_2 & y - \sin(\theta_1)l_2 \\ x - l_1 & y \end{bmatrix} \tag{14}$$

$$\mathbf{B_I} = \begin{bmatrix} \sin(\theta_1)l_2x - \cos(\theta_1)l_2y & 0 \\ 0 & r \end{bmatrix} \tag{15}$$

While for the second actuation scheme (II), the expressions of Jacobian matrices $\mathbf{A_{II}}$ and $\mathbf{B_{II}}$ are as follows:

$$\mathbf{A_{II}}\begin{bmatrix}\dot{x}\\ \dot{y}\end{bmatrix} = \mathbf{B_{II}}\begin{bmatrix}\dot{\theta_1}\\ \dot{\theta_2}\end{bmatrix} \tag{16}$$

$$\mathbf{A_{II}} = \begin{bmatrix} x - \cos(\theta_1)l_2 & y - \sin(\theta_1)l_2 \\ -\sin(\theta_2) & \cos(\theta_2) \end{bmatrix} \tag{17}$$

$$\mathbf{B_{II}} = \begin{bmatrix} (\sin(\theta_1)l_2x & 0 \\ -\cos(\theta_1)l_2y) & \\ & ((l_1 - x)\cos(\theta_2) \\ 0 & y\sin(\theta_2)) \end{bmatrix} \tag{18}$$

The mechanism will suffer Type 1 singularity if the determinant of matrix A is null, i.e.$\det(\mathbf{A_I}) = 0$ and $\det(\mathbf{A_{II}}) = 0$. Consequently, the mechanism loses one or more motions. Likewise, the mechanism will be subjected to the Type 2 singularity is the determinant of matrix B is null, i.e.$\det(\mathbf{B_I}) = 0$ and $\det(\mathbf{B_{II}}) = 0$. As a consequence, the mechanism motions become uncontrollable.

3.4. Transmission Angles and Transmission Indices

Transmission angle in a linkage may signify the quality of force transmission and it will affect the mechanical efficiency. As a consequence, the selection of actuated joint in a linkage has a great influence on the transmission angle. Transmission angles can also indicate whether the linkage is subjected to either Type 1 or Type 2 singularities.

The quality of force transmission for five-bar linkage under study is defined by two transmission angles ϕ_1 and ϕ_2, as shown in Figure 4. As the linkage moves, the transmission angles and all other joints angles constantly change. According to Section 3.2, link ABP has two configurations as: solution 1 and solution 2. Therefore, there are two possibilities of transmission angles. The transmission angles for solution 1 configuration are as follows:

$$\phi_1 = \cos^{-1}\left(\frac{{l_3}^2 + {l_2}^2 - {l_1}^2 - r^2 + 2l_1r\cos(\pi - \theta_1)}{2l_3l_2}\right) \tag{19}$$

$$\phi_2 = \cos^{-1}\left(\frac{{l_3}^2 + r^2 - {l_1}^2 - {l_2}^2 + 2l_1l_2\cos(\theta_1)}{2l_3r}\right) \tag{20}$$

and the transmission angles for solution 2 configuration are as follows:

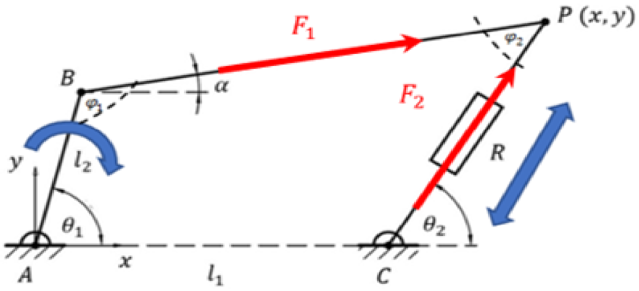

(a) Actuation scheme I

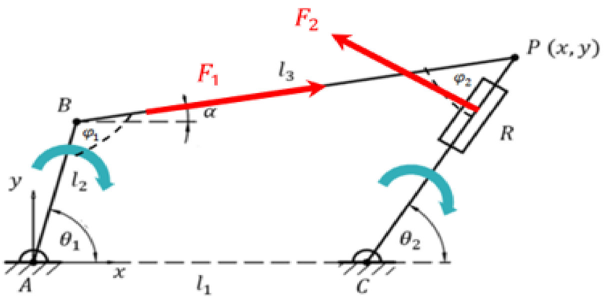

(b) Actuation scheme II

Figure 4. Distribution of actuation forces (a) Actuation scheme I, (b) Actuation scheme II

$$\phi_2 = \cos^{-1}\left(\frac{{l_2}^2 + {l_3}^2 - {l_1}^2 - r^2 + 2l_1 r cos\,(\pi - \theta_2)}{2l_2 l_3}\right) \tag{21}$$

$$\phi_2 = \cos^{-1}\left(\frac{{l_2}^2 + {l_3}^2 - {l_1}^2 - r^2 + 2l_1 r cos\,(\pi - \theta_2)}{2l_2 l_3}\right) \tag{22}$$

If angle ϕ_1 is at 0° or 180° for both actuation schemes, link ABP is in the Type 1 singularity. As a consequence, link ABP cannot be moved and loses its mobility. If angle ϕ_2 is at 0° or 180° for the first actuation scheme, two actuation forces F_1 and F_2 are collinear. It means that the linkage does not transmit any force to the output point P and is subjected to Type 2 singularity. In this configuration, the linkage will have a shaky motion. For the second actuation scheme, two forces F_1 and F_2 are collinear if the angle ϕ_2 is at 90°. In this configuration, the linkage cannot transmit any force hence the linkage will have shaky motion. The linkage will be at optimum condition for both actuation schemes whenever the transmission angles ϕ_1 and ϕ_2 do not meet the abovementioned values.

For design purposes, the transmission angles are converted into the transmission indices; hence their values can be bounded within 0 and 1. For solution 1 configuration, the transmission indices are:

$$\kappa_1 = \cos\,(\phi_1), \quad \kappa_2 = \cos\,(\phi_2), \quad \kappa_1,\ \kappa_2 \in [0, 1] \tag{23}$$

For solution 2 configuration, the transmission indices are:

$$\lambda_1 = \cos\,(\phi_1), \quad \lambda_2 = \sin\,(\phi_2), \quad \lambda_1,\ \lambda_2 \in [0, 1] \tag{24}$$

These transmission indices will be used for the optimization process which will be described hereafter.

4. Optimization Problem

In this paper, a Pareto optimal solution is employed for the design optimization process to produce a set of equally valid solutions. Thus, the optimization aims to determine and propose a set of five-bar linkage designs that simultaneously minimize the transmission indices. Therefore, the design problem can be formulated for Solution 1 configuration as follows:

$$\begin{array}{rcc} minimize & : & (\kappa_1)\ and\ (\kappa_2) \\ over & : & [l_1 \quad l_2 \quad l_3 \quad \theta_1 \quad \theta_2 \quad R \quad] \end{array} \tag{25}$$

For Solution 2 configuration, the design problem is defined as follows:

$$\begin{array}{rcc} minimize & : & (\lambda_1)\ and\ (\lambda_2) \\ over & : & [l_1 \quad l_2 \quad l_3 \quad \theta_1 \quad \theta_2 \quad R \quad] \end{array} \tag{26}$$

5. KASITS: A Graphical User Interface

Based on the analysis of direct kinematics, inverse kinematics, singularities and the optimization problems, a new graphical user interface is developed. This interface is named KASITS (Kinematic Analysis and Synthesis of ITS) for the kinematic analysis and synthesis of five-bar linkage with prismatic joint. The picture of five-bar linkage with prismatic joint is provided in KASITS to give visual illustration to the users. The initial step for the users is to choose whether they intend to carry out kinematic analysis or synthesis by clicking on the "analysis" or "synthesis" button. In what follows, we explain the steps provided in analysis and synthesis menus.

5.1. Analysis

By clicking the analysis button, the new window will appear as shown in Figure 5(a). To start the analysis, the users may conduct the following procedures:

1. Design parameter Input the value of design parameter l_1, l_2, l_3
2. Actuation scheme Select which actuation scheme will be analyzed.
3. Actuated joint limit Input the value of actuated joint limits that correspond to the selected actuation scheme.
4. Click "generate" to show the analysis results. The plot of workspace and singularity will appear.
5. Click "Solution 1" or "Solution 2" to show the linkage configurations.
6. Click "Type 1" or "Type 2" to show the linkage configuration at singularity.
7. Click "Clear" to start over.

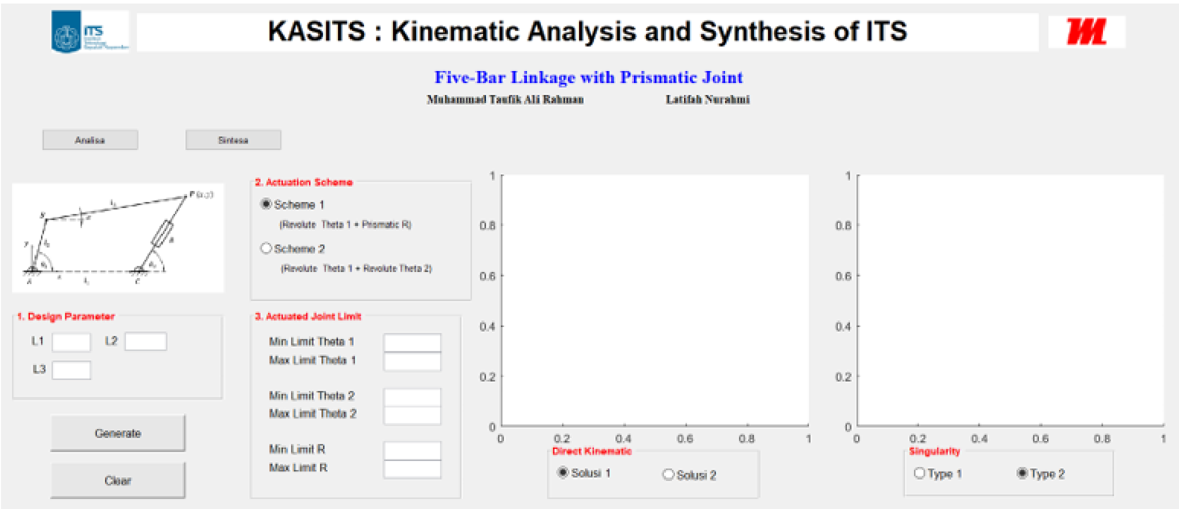

(a) Analysis window

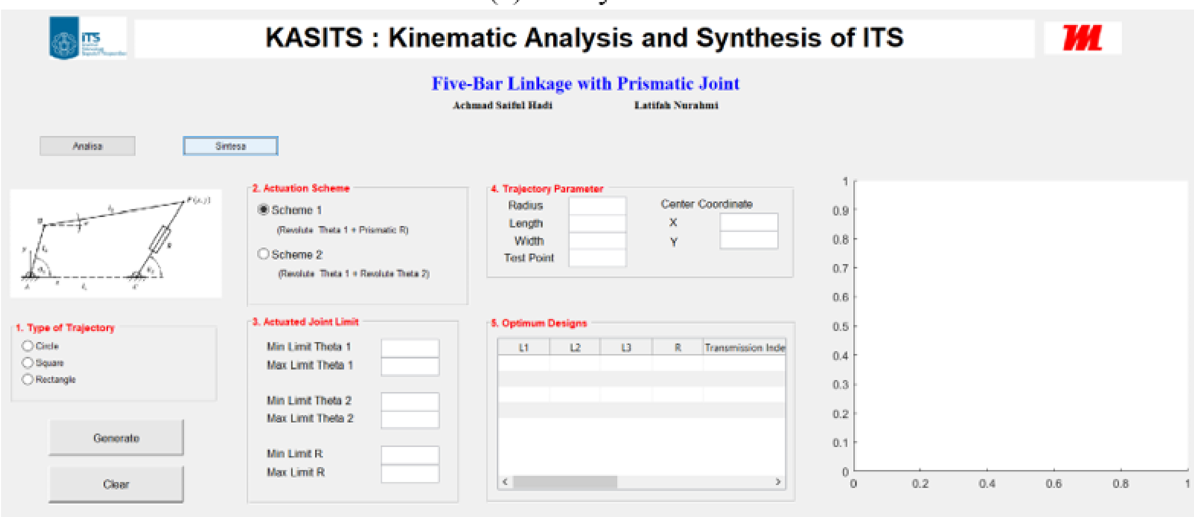

(b) Synthesis window

Figure 5. Graphical users interface KASITS (a) Analysis window, (b) Synthesis window

5.2. Analysis

By clicking the synthesis button, the new window will appear as shown in Figure 5(b). To start the synthesis, the users may carry out the following procedures:

1. Type of trajectory The users may select which type of trajectory they want to achieve. There are three types of trajectory, namely circle, square and rectangle.

2. Actuation scheme Select which actuation scheme will be analyzed.

3. Actuated joint limit Input the value of actuated joint limits that correspond to the selected actuation scheme.

4. Trajectory parameter Input the value of parameters and the number of test point for the corresponding trajectory.

5. Click "generate" to show the synthesis results. The pareto graph will be shown and a set of optimum designs l_1, l_2, l_3 will appear in table.

6. Click "Clear" to start over.

6. Applications of KASITS

6.1. Kinematics Analysis

In this section, KASITS will be used to analyze the workspace and singularities of five-bar linkage with prismatic joint. The values of design parameters are substituted as $l_1 = 8$,$l_2 = 4$,$l_3 = 12$. The first actuation scheme is selected and the actuated joint limits are set as $0° \leq \theta_1 \leq 360°$ and $1 \leq R \leq 8$.

"Generate" button is clicked and the results are shown in Figure 6. The blue surface describes all points in Cartesian coordinates which can be attained by point P while the linkage is at Solution 1 configuration. Likewise, the red surface shows all points in Cartesian coordinates which can be reached by point P when the linkage is at Solution 2 configuration. The green curve shows the Type 2 singularity.

6.2. Kinematics Synthesis

KASITS can also be used to carry out the kinematic synthesis of five-bar linkage with prismatic joint. The initial step is to choose which trajectory should be accomplished by point P. In the following application, a circle trajectory is selected with radius 2 of center (5,6) and test point 20 discrete points. The first actuation scheme is chosen with actuated joint limit as $10° \leq \theta_1 \leq 95°$, dan $4 \leq R \leq 8.5$.

The "Generate" button is clicked and the results are shown in Figure 7. All possible designs of five-bar linkage with prismatic joint are plot in the graph of Pareto Optimal Solutions as red and yellow dots. The red and yellow dots represent the Solution 1 and Solution 2 configurations, respectively. The optimum designs are the ones with the blue circle and pointed out by the blue arrows in Figure 8.

According to optimization plot in Figure 8, there are 11 optimum designs that minimize both objective functions. However, some designs among 11 optimum designs are the same, thus they are automatically eliminated by the GUI. Eventually, it remains 7 independent optimum designs shown in GUI.

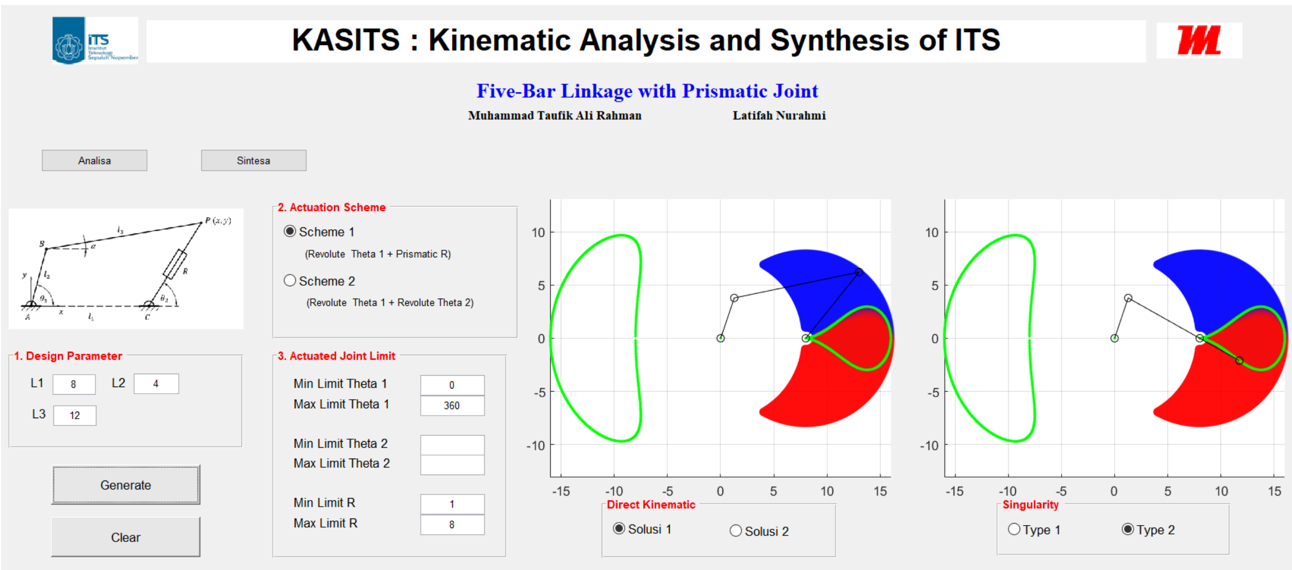

Figure 6. Application of KASITS for kinematic analysis

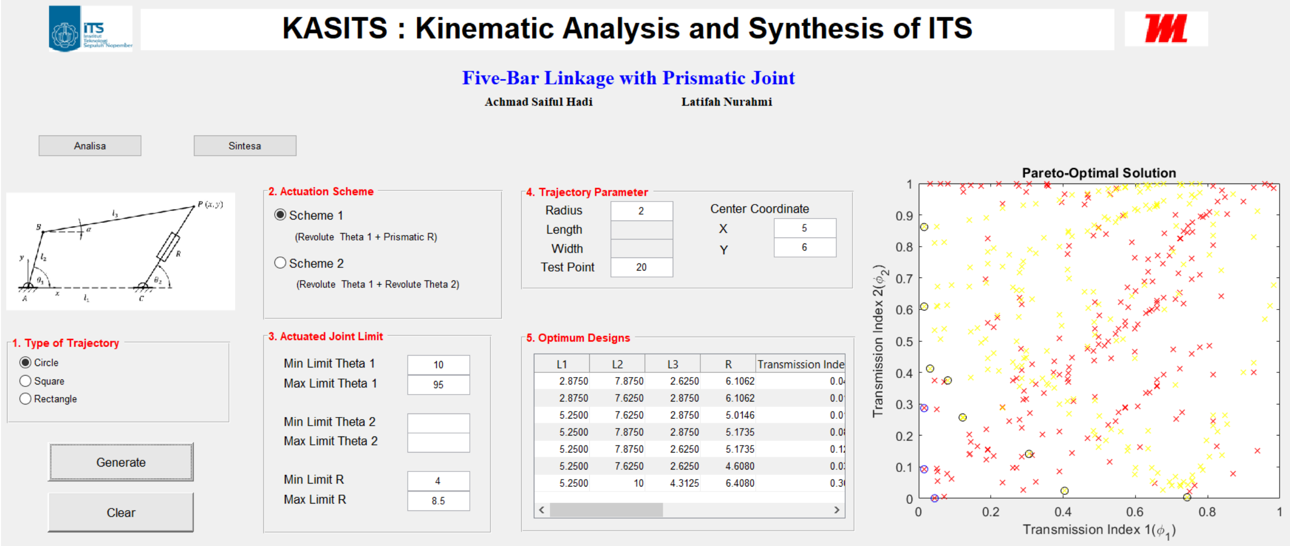

Figure 7. Application of KASITS for kinematic synthesis

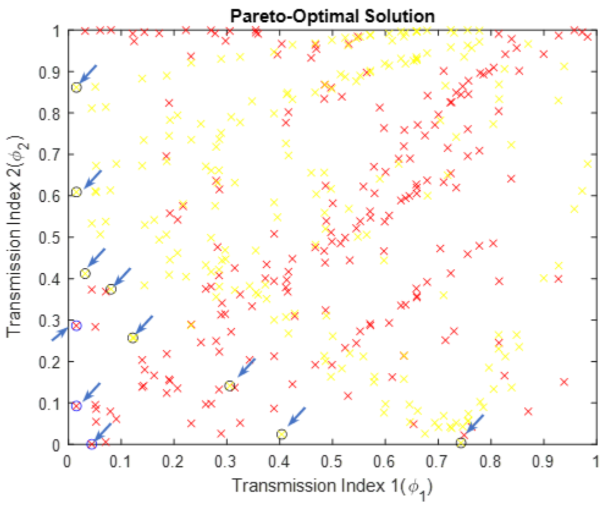

Figure 8. Pareto Optimal Solutions from GUI

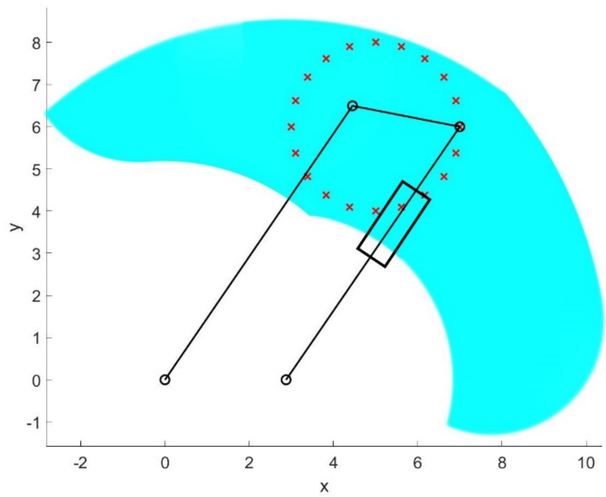

Figure 9. Selected optimum design of five-bar linkage with prismatic joint

To give physical interpretation of one optimum design, the first design from table in GUI is considered. This design shows that the linkage has $l_1 = 2.875$,$l_2 = 7.8750$,$l_3 = 2.6250$. The workspace of this linkage is plotted and the circle trajectory is located inside the workspace as shown in Figure 9. It confirms that the selected design can achieve the given circle trajectory.

7. Conclusions

A new graphical user interface, named KASITS (Kinematic Analysis and Synthesis of ITS), was proposed in this paper. It allows the users to analyze and synthesize a five-bar linkage with prismatic joint conveniently. The analysis was based on the computation of direct kinematics. Given the value of design parameters, the interface will plot the workspace shape or the collection of points which can be attained by the linkage. Moreover, the singularity curve will also be shown inside its workspace based on the vanishing condition of Jacobian determinant. The linkage synthesis was based on the inverse kinematics and optimization process. Given the trajectory, the value of design parameters was traced by the interface to determine a list of optimum designs. These optimum designs fulfill the minimum conditions of transmission indices.

References

[1] D. Mundo, G. Gatti, and D. Dooner, "Optimized five-bar linkages with non-circular gears for exact path generation," *Mechanism and Machine Theory*, vol. 44, no. 4, pp. 751–760, 2009.

[2] L. Campos, F. Bourbonnais, I. A. Bonev, and P. Bigras, "Development of a five-bar parallel robot with large workspace," in *International Design Engineering*

Technical Conferences and Computers and Information in Engineering Conference, vol. 44106, pp. 917–922, 2010.

[3] T. D. Le, H.-J. Kang, and Y.-S. Ro, "Kinematic and singularity analysis of symmetrical 2 dof parallel manipulators," in *2012 7th International Forum on Strategic Technology (IFOST)*, pp. 1–4, IEEE, 2012.

[4] M. Koçak, F. C. Can, and E. Gezgin, "Design of a graphical user interface for the structural synthesis of parallel manipulators with single platform," in *International Conference on Interactive Collaborative Robotics*, pp. 182–192, Springer, 2019.

[5] S. Zodey and S. K. Pradhan, "Matlab toolbox for kinematic analysis and simulation of dexterous robotic grippers," *Procedia Engineering*, vol. 97, pp. 1886–1895, 2014.

[6] L. Nurahmi, J. Schadlbauer, S. Caro, M. Husty, and P. Wenger, "Kinematic analysis of the 3-rps cube parallel manipulator," *Journal of Mechanisms and Robotics*, vol. 7, no. 1, 2015.

[7] L. Nurahmi, S. Caro, and M. Solichin, "A novel ankle rehabilitation device based on a reconfigurable 3-rps parallel manipulator," *Mechanism and Machine Theory*, vol. 134, pp. 135–150, 2019.

[8] L. Nurahmi and D. Gan, "Reconfiguration of a 3-(rr) ps metamorphic parallel mechanism based on complete workspace and operation mode analysis," *Journal of Mechanisms and Robotics*, vol. 12, no. 1, 2020.

[9] S. Amine, M. T. Masouleh, S. Caro, P. Wenger, and C. Gosselin, "Singularity analysis of 3t2r parallel mechanisms using grassmann–cayley algebra and grassmann geometry," *Mechanism and Machine Theory*, vol. 52, pp. 326–340, 2012.

[10] S. Amine, S. Caro, P. Wenger, and D. Kanaan, "Singularity analysis of the h4 robot using grassmann–cayley algebra," *Robotica*, vol. 30, no. 7, pp. 1109–1118, 2012.

[11] S. Amine, L. Nurahmi, P. Wenger, and S. Caro, "Conceptual design of schoenflies motion generators based on the wrench graph," in *ASME 2013 International Design Engineering Technical Conferences and Computers and Information in Engineering Conference*, American Society of Mechanical Engineers Digital Collection, 2013.

[12] S. Caro, L. Nurahmi, and P. Wenger, "Graphical user interface for the singularity analysis of lower-mobility parallel manipulators," in *New Trends in Mechanism and Machine Science*, pp. 21–30, Springer, 2015.

[13] A. Selvakumar, "Singularity analysis of 3 dof parallelmanipulators for angular drilling in medicalapplications," *International Journal of Engineering and Advanced Technology (IJEAT), Volume-9 Issue-1S3*, pp. 461–465, 2019.

[14] M. T. Hoang, T. T. Vuong, and C. B. Pham, "Study and development of parallel robots based on 5-bar linkage," pp. 21–30, 2015.

[15] L. Nurahmi, S. Caro, and S. Briot, "Type synthesis of two dof hybrid translational manipulators," in *Computational Kinematics*, pp. 249–259, Springer, 2014.

[16] K. H. Hunt, K. H. Hunt, and K. H. Hunt, *Kinematic geometry of mechanisms*, vol. 7. Oxford University Press, USA, 1978.

[17] C. Germain, S. Caro, S. Briot, and P. Wenger, "Singularity-free design of the translational parallel manipulator irsbot-2," *Mechanism and Machine Theory*, vol. 64, pp. 262–285, 2013.